

BEAM OPTIMIZATION AND MEASUREMENT OF CAEP FEL-THz INJECTOR*

D. Wu, D. X. Xiao, P Li, J. X. Wang[†], X. K. Li, X. Luo, K. Zhou, C. L. Lao,
Q. Pan, S. F. Lin, L. J. Shan, H. B. Wang, X. F. Yang, M. Li
Institute of Applied Electronics, China Academy of Engineering Physics (CAEP/IAE),
Mianyang, P. R. China

Abstract

The FEL-THz facility in Chinese Academy of Engineering Physics (CAEP) requires high brightness high repetition electron beam, which needs optimization of multi-parameter and multi-objective, such as emittance, energy spread, bunch length, etc. In this paper, some studies of beam optimization based on differential evolution (DE) algorithm and Astra code are shown. Dozens of the DC-SRF-injector parameters have been considered in the optimization. Some measurements of the electron beam are also introduced, including emittance measurement with the three-profile method, energy spread measurement with analyzing magnet and beam length diagnostics with zero-phasing method. These studies indicate that the injector beam quality satisfies the requirement of the FEL-THz facility.

INTRODUCTION

High average power high-brightness electron source plays a significant role in the path to the realization of the future high repetition short-wave free electron lasers (FELs) and energy recovery linacs (ERLs)[1, 2]. With the construction of European XFEL[3], and with some new projects put forward, such as LCLS-II[4] and MaRIE[5], the X-ray free electron lasers are moving in the direction of high repetition or even continuous-wave mode. These new developments have proposed some new requirements of the high brightness electron sources. The biggest challenge is to maintain the high brightness (electron charge ~ 200 pC, emittance < 0.5 mm-mrad, longitudinal length < 1 ps and energy spread $\sim 10^{-5}$) of the electron beams at high average current (\sim MHz repetition and ~ 100 mA average current).

High-voltage (HV) DC photocathode injector with superconducting RF accelerator could provide high brightness electron beams in CW mode, which makes it a hotspot in short-wave FEL research. One of the best results[6] is achieved by CLASS team in Cornell university, who has get a 0.3 mm-mrad emittance (95% core) at 100 pC CW mode with 1.3 GHz repetition. The dynamics design of the Cornell beamline is optimized by a multivariate genetic algorithm[7].

In China, the CAEP FEL-THz facility is the first high average Tera-Hertz source based on FEL, which is driven by

a DC gun with GaAs photocathode and two 4-cell 1.3 GHz super-conducting radio frequency (SRF) accelerator[8–12]. This is also the first DC-SRF-injector designed for high-Brightness electron beams In China. The repetition of FEL-THz is 54.167 MHz, one in twenty-fourth of 1.3 GHz. The effective accelerator field gradient is about 10 MV/m. The injector could provide high-brightness CW electron beam for the oscillator Tera-Hertz free electron laser. And the beam quality could be optimized better than the FEL-THz requirements. In this paper, an optimization with differential evolution genetic algorithm is discussed. And the beam measurement is shown, including emittance, energy spread and bunch length.

BEAM OPTIMIZATION

DE Algorithm

Differential evolution (DE) algorithm is a heuristic global optimization based on population, works on Darwin's concept of survival of the fittest[13, 14]. DE and other evolutionary algorithms are often used to solve the beam dynamic optimization[7, 15–17]

DE starts with a population of NP candidate solutions, which may be represented as $X_{i,G}$, $i = 1, 2, \dots, NP$, where i index denotes the population and G denotes the generation to which the population belongs. DE uses mutation, crossover and selection to solve problems, which are shown in Fig. 1.

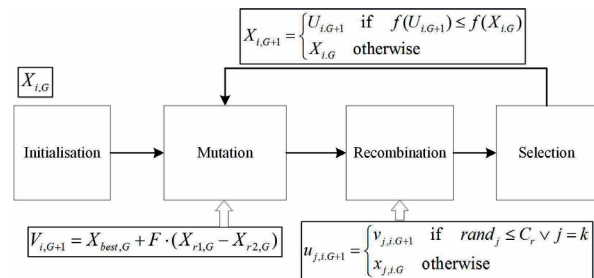


Figure 1: DE flow chart.

The mutation operator is the prime operator of DE. In this paper, a so-called 'best-strategy-type-1' is used[18], where $F \in [0, 1]$ is the control parameter. $r_i \in \{1, \dots, NP\}$ is a random selection and $r_1 \neq r_2$. The operator recombination and selection are also shown in Fig. 1 The crossover rate $C_r \in [0, 1]$ is the other control parameter of DE.

The most important part in the selection operator is the objective function f . In the one-objective situation, f is often as simple as normalized emittance or energy spread

* Work supported by China National Key Scientific Instrument and Equipment Development Project (2011YQ130018), National Natural Science Foundation of China with grant (11475159, 11505173, 11576254 and 11605190)

[†] jianxinwang1026@163.com

Content from this work may be used under the terms of the CC BY 3.0 licence (© 2017). Any distribution of this work must maintain attribution to the author(s), title of the work, publisher, and DOI.

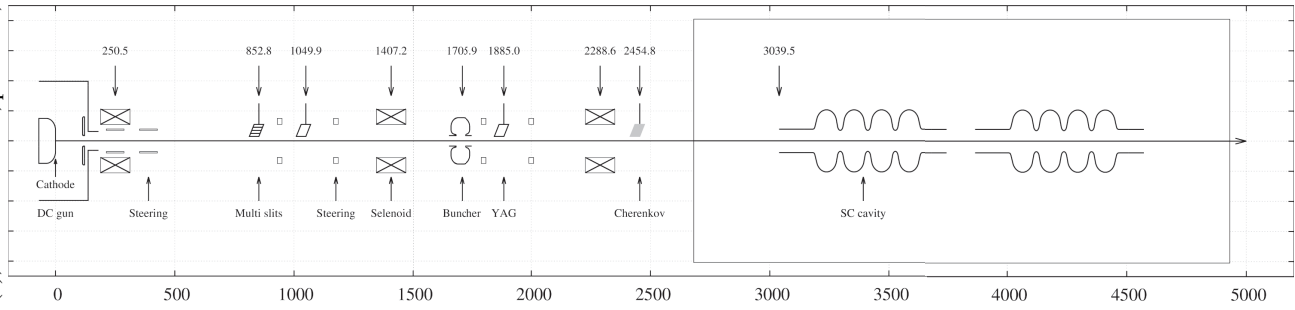


Figure 2: The layout of FEL-THz photo-injector(unit:mm).

in a specific location. But the beam optimization is a multi-objective problem, which means many parameters should be considered together, such as emittance, energy spread, bunch length and transverse beam size. In this paper, two linear objective functions are considered as:

$$f(x) = \sum_i \omega_i f_i(x) \quad \text{or} \quad f(x) = \sum_i \omega_i \left| \frac{f_i(x) - f_{i,0}}{f_{i,0}} \right| \quad (1)$$

where $\omega_i > 0$ is artificially given parameters to highlight main goal. In the left function the magnitude of each objective should be estimated in advance. Its advantage is to be able to search for a better solution than expected. The right one have an ideal solution when $f_i = f_{i,0}$, where $f_{i,0}$ is the preset target for each goal.

Optimization Results

The location of injector elements are shown in Fig. 2. There are three solenoids and one RF buncher upstream of the 2x4-cell superconducting RF accelerator. The first solenoid is used for the emittance compensation[19]. The second and the third ones are used to adjust the transverse beam size before the buncher and accelerator, respectively.

The range of design parameters are shown in Table 1. B_{s1} is the center magnetic field along beamline. $E_{b,avg}$ is the average electric field gradient of the buncher. ϕ_b and ϕ_{sc} are the phase of buncher and accelerators, respectively. The gradient of SC accelerator is preset as 8 MV/m. The beam dynamics is simulated by ASTRA code[20], in which the relative phase is used, making $\phi = 0$ the maximum accelerating phase. σ_r is the RMS beam size on the cathode with a two-dimension Gaussian distribution, the lower limit of which is given by the space charge limit (SCL)[21]:

$$\sigma_{r,min,gaussian} = \sqrt{\frac{Q}{2\pi\epsilon_0 E_0}} \quad (2)$$

where Q is the beam charge and E_0 the electric field gradient on the cathode.

The objective function is to minimize the emittance, bunch length, energy spread at the exit of the accelerator, in which the emittance has the largest weighting factor ω . One

of the results is shown in Fig. 3, where (a) is the convergence process of every individual's normalized emittance (unit:mm-mrad) in generations. (b)-(f) are the normalized emittance, the transverse RMS beam size, the longitudinal FWHM length, the energy spread and the kinetic energy along the beam direction z , respectively.

Table 1: Range of Design Parameters

Parameter/Unit	Lower limit	Upper limit
σ_r /mm	0.66	2
B_{s1} /Gs	240	320
B_{s2} /Gs	90	200
B_{s3} /Gs	90	200
$E_{b,avg}$ /MV·m ⁻¹	0.6	2
ϕ_b /deg	-110	-70
ϕ_{sc1} /deg	-20	10
ϕ_{sc2} /deg	-20	20

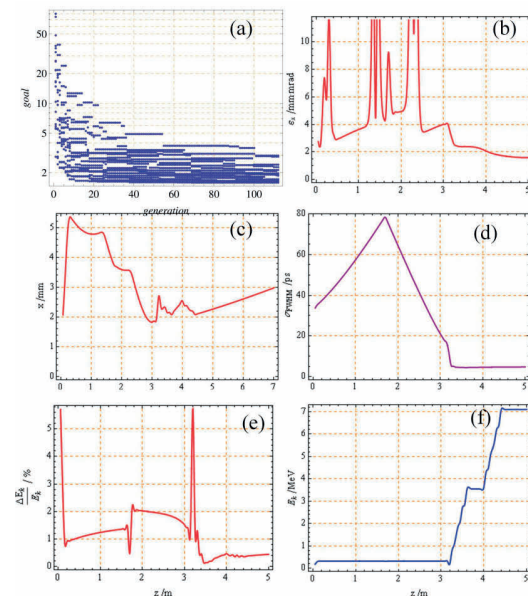


Figure 3: One optimization result with DE algorithm.

The optimization in 100 generations shows that the emittance can be 1.86 mm-mrad and other parameters can also meet the requirements of FEL-THz facility when $Q=92$ pC, $\sigma_r=0.7$ mm, $B_{s1}=278$ Gs, $B_{s2}=121$ Gs, $B_{s3}=149$ Gs, $E_{b,avg}=1.2$ MV/m, $\phi_b=-85^\circ$, $\phi_{sc1}=-10^\circ$ and $\phi_{sc2}=-5^\circ$.

BEAM MEASUREMENT

Emittance

The three-profile method[22] is used to measure the emittance downstream of the accelerator. The transverse beam distribution and the normalized emittance are shown in Fig. 4 and Table. 2. The result is larger than the simulation because of space charge force and low beam energy.

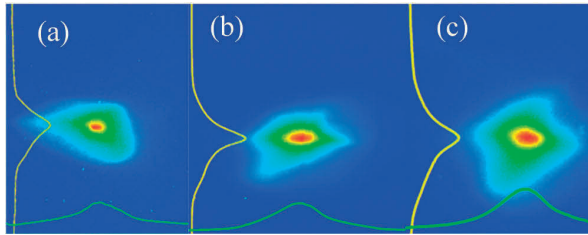


Figure 4: The three profiles for emittance measurement.

Table 2: Emittance measurement result

σ_{xa}	σ_{xb}	σ_{xc}	l_{ab}	l_{bc}	E_k	$\epsilon_{n,x}$
1.53	1.07	1.01	1662	2503	8.1	8.2
mm	mm	mm	mm	mm	MeV	mm-mrad

Energy Spread

Fig. 5 shows the energy spread versus buncher field scanning. There is a 90° analysis magnetic system with a slit and a YAG screen. The distance between the slit and the magnet is 300mm, the same as the one between the magnet and the creen. The buncher field is measured by the pickup power. The E_b in this picture presents the peak field and is much larger than the simulation. The minimized FWHM energy spread is 0.3% when the peak field $E_b=1.7$ MV/m.

Bunch Length

The beam bunch length is measured with zero-phasing method[23, 24]. Because the length change is small after the first 4-cell SC cavity according to the simulation, the second 4-cell one is used to measure the bunch length, making the kinetic energy much smaller than the full power operation. Fig. 6 (a)-(c) are the energy spread when the second 4-cell accelerator is turn-off, in the rising zero phase and in the descending zero phase, respectively. (d)-(f) are the projection of the images (a)-(c) in x direction. The second peak in Fig. 6 (d) is due to the ghost pulses which should be ignored.

Solve the following equation and the bunch length can be achieved in Table. 3. The result is larger than the simulation

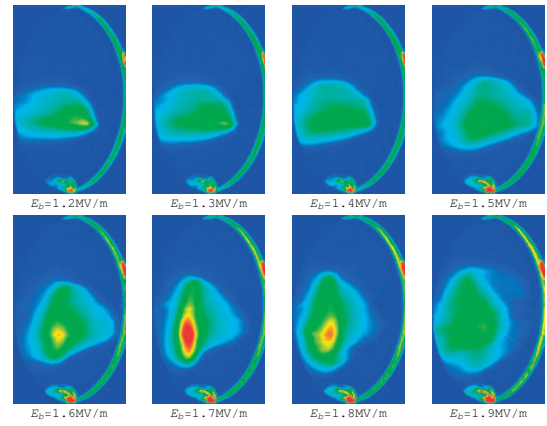


Figure 5: Energy spread scanning.

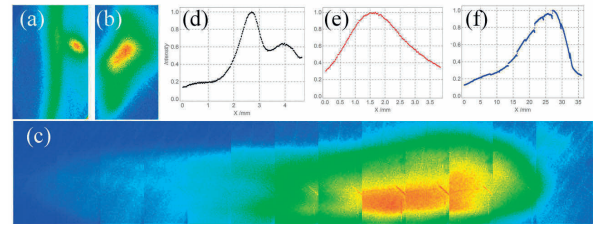


Figure 6: Energy distribution for zero-phasing method

also because of space charge force and low beam energy.

$$\sigma_x = \sqrt{\sigma_{x0}^2 + \sigma_z^2 \eta^2 \left[\frac{1}{E_0} \left(\frac{dE}{dz} \right)_0 + \frac{2\pi e V_{rf}}{\lambda_{rf} E_0} \right]^2} \quad (3)$$

Table 3: Bunch Length Measurement Result

σ_{x0}	$\sigma_{x,0}$	$\sigma_{x,\pi}$	E_0	λ_{rf}	η	σ_z
0.5	0.94	8.05	3.1	0.23	0.3	0.94
mm	mm	mm	MeV	m	m	mm

SUMMARY

In this paper, the simulation optimization with differential evolution algorithm and ASTRA code are introduced. The emittance of the FEL-THz photo-injector can be reduced to less than 2 mm-mrad, with all the other beam parameters meet the facility requirements. The normalized emittance is measured as 8.2 mm-mrad with 3-profile method. The energy spread is proved to be as small as 0.3%. And a 0.94 mm RMS bunch length is measured by the means of zero-phasing method. This research indicates that DE algorithm is effective on the beamline optimization, and all the beam micro-pulse parameters fulfil the requirements of FEL-THz facility.

REFERENCES

- [1] D. Dowell *et al.*, “Cathode r&d for future light sources,” *Nuclear Instruments and Methods in Physics Research Section A: Accelerators, Spectrometers, Detectors and Associated Equipment*, vol. 622, no. 3, pp. 685–697, 2010.
- [2] T. Rao and D. H. Dowell, *An engineering guide to photoinjectors*. 2014.
- [3] M. Altarelli *et al.*, “The European X-ray free-electron laser,” DESY, Tech. Rep., 2006, pp. 1–26.
- [4] J. N. Galayda, “The LCLS-II project,” Tech. Rep., 2014.
- [5] J. Lewellen *et al.*, “Status of the MaRIE X-FEL accelerator design,” in *Proceedings of IPAC’15*, Richmond, VA, USA, 2015, pp. 1894–1896.
- [6] A. Bartnik, C. Gulliford, I. Bazarov, L. Cultera, and B. Dunham, “Operational experience with nanocoulomb bunch charges in the cornell photoinjector,” *Physical Review Special Topics-Accelerators and Beams*, vol. 18, no. 8, p. 083401, 2015.
- [7] I. Bazarov and C. Sinclair, “Multivariate optimization of a high brightness DC gun photoinjector,” *Physical Review Special Topics - Accelerators and Beams*, vol. 8, no. 3, p. 034202, 2005.
- [8] P. Li, Y. Jiao, W. Bai, H. B. Wang, X. H. Cui, and X. K. Li, “Start-to-end simulation of CAEP FEL-THz beamline,” *High Power Laser and Particle Beams*, vol. 26, no. 8, p. 083102, 2014.
- [9] M. Zheng-Hui *et al.*, “Design and test of frequency tuner for a CAEP high power THz free-electron laser,” *Chinese Physics C*, vol. 39, no. 2, p. 028102, 2015.
- [10] X. Luo *et al.*, “Design and fabrication of the 2×4-cell superconducting linac module for the free-electron laser,” *Nuclear Instruments and Methods in Physics Research Section A: Accelerators, Spectrometers, Detectors and Associated Equipment*, vol. 871, pp. 30–34, 2017.
- [11] K. Zhou *et al.*, “Progress of the 2×4-cell superconducting accelerator for the CAEP THz-FEL facility,” in *Proceedings of the 18th International Conference on RF Superconductivity*, Lanzhou China, Jul. 2017, unpublished.
- [12] X. Luo *et al.*, “Design of the 2×4-cell superconducting cryomodule for the free-electron laser,” in *Proceedings of the 18th International Conference on RF Superconductivity*, Lanzhou, China, Jul. 2017, unpublished.
- [13] R. Storn and K. Price, “Differential evolution—a simple and efficient heuristic for global optimization over continuous spaces,” *Journal of global optimization*, vol. 11, no. 4, pp. 341–359, 1997.
- [14] M. Ali, M. Pant, and A. Abraham, “A simplex differential evolution algorithm: Development and applications,” *Transactions of the Institute of Measurement and Control*, vol. 34, no. 6, pp. 691–704, 2012.
- [15] J. Qiang, Y. Chao, C. Mitchell, S. Paret, and R. Ryne, “A parallel multi-objective differential evolution algorithm for photoinjector beam dynamics optimization,” in *Proceedings of IPAC’13*, 2013, pp. 1031–1033.
- [16] Y. Zhang and D. Zhou, “Application of differential evolution algorithm in future collider optimization,” in *7th International Particle Accelerator Conference (IPAC’16)*, Busan, Korea, May 8-13, 2016, JACOW, Geneva, Switzerland, 2016, pp. 1025–1027.
- [17] L. Y. Zhou *et al.*, “Design of an X-band photocathode rf gun for tsinghua thomson scattering X-ray source,” in *IPAC’17*, 2017, pp. 1025–1027.
- [18] W. Gong, A. Fialho, and Z. Cai, “Adaptive strategy selection in differential evolution,” in *Proceedings of the 12th annual conference on Genetic and evolutionary computation*, ACM, 2010, pp. 409–416.
- [19] B. Carlsten, “Space-charge-induced emittance compensation in high-brightness photoinjectors,” in *PAC’95*, vol. 49, 1995, pp. 27–65.
- [20] K. Flöttmann, “Astra: A space charge tracking algorithm,” *Manual, Version*, vol. 3, 2011.
- [21] J. Rosenzweig *et al.*, “Initial measurements of the ucla RF photoinjector,” *Nuclear Instruments and Methods in Physics Research Section A: Accelerators, Spectrometers, Detectors and Associated Equipment*, vol. 341, no. 1-3, pp. 379–385, 1994.
- [22] R. Cutler, J. Owen, and J. Whittaker, “Performance of wire scanner beam profile monitors to determine the emittance and position of high power cw electron beams of the nbs-los alamos racetrack microtron,” in *Proceedings of the 1987 IEEE particle accelerator conference: Accelerator engineering and technology*, 1987.
- [23] D. X. Wang, G. A. Krafft, and C. K. Sinclair, “Measurement of femtosecond electron bunches using a rf zero-phasing method,” *Phys. Rev. E*, vol. 57, pp. 2283–2286, 2 Feb. 1998.
- [24] W. Graves *et al.*, “Ultrashort electron bunch length measurements at DUVFEL,” in *PAC’01*, vol. 3, 2001, pp. 2224–2226.